American Journal of Optics and Photonics
2016; 4(5): 40-45
http://www.sciencepublishinggroup.com/j/ajop
doi: 10.11648/j.ajop.20160405.11
ISSN: 2330-8486 (Print); ISSN: 2330-8494 (Online)

First Investigation of Optical Properties and Local Structure of Gd^{3+} Doped Nano-Crystalline $GeSe_2$

H. Hantour

Faculty of Science, Al-Azhar University, Cairo, Egypt

Email address:
hananhantourmy@yahoo.com

To cite this article:
H. Hantour. First Investigation of Optical Properties and Local Structure of Gd^{3+} Doped Nano-Crystalline $GeSe_2$. *American Journal of Optics and Photonics*. Vol. 4, No. 5, 2016, pp. 40-45. doi: 10.11648/j.ajop.20160405.11

Received: October 31, 2016; **Accepted**: November 12, 2016; **Published**: November 29, 2016

Abstract: Pure and Gd-doped nano-crystalline $GeSe_2$ were prepared by the melt-quenching technique. The crystal structure, local structure and emission properties are investigated. Structure analysis using Rietveld program suggests monoclinic structure for both virgin and doped samples with nano-particle size 41nm for $GeSe_2$ and 48nm for Gd-doped sample. A wide optical band gap as estimated from absorbance measurements is 4.1ev and 4.8ev for pure and doped samples in accordance with the confinement effects. Raman spectra show two unresolved components at ~ 202 cm^{-1} with broad line width. Also, well identified low intensity (υ < 145 cm^{-1}) and high intensity (υ > 250 cm^{-1}) bands are detected. For Gd-doped sample, the main band is shifted to lower energies and its FWHM is reduced by ~ 50% accompanied by an intensity increase of about ~ 17 fold times. The photoluminescence analysis of the pure sample shows a main emission band at ~ 604 nm. This band is splitted into two separated bands with higher intensity. The detected emission bands at wavelength > 650 nm are assigned to transmission from ^6G_J to the different ^6P_J terms.

Keywords: Nano-Crystalline $GeSe_2$Doped with Gd^{3+}, Microstructure, Optical, Raman and Photoluminescence Characteristics

1. Introduction

Chalcogenides based Ge-Selenides have significant infrared (IR) transparency in the wavelength region between ~1 and 12μm which makes them suitable for passive IR optics, for example as optical fibers, wave guides, sensors, nano-lens and photo-resist materials for the micro and nano fabrication [1-6]. Various works have been reported on the Ge-Se system chemically modified by addition of I-VII group elements of the periodic table [7-9].

Rare-earth doped chalcogenides havebeen studied in recent years for active applications in the near- and mid- IR [10, 11]. The primary advantage for choosing a chalcogenide host is the smaller phonon energy (~ 350 cm^{-1} for selenides) as compared to fluoride (~ 550 cm^{-1}) and silicate (~ 1100 cm^{-1}) hosts. This smaller phonon energy results in a smaller multiphonon transition probability thereby allowing mid-IR transitions normally quenched in the larger phonon energy hosts to become active [12, 13].

Raman spectroscopy has been an important tool for investigating the properties of chalcogenide materials. A large number of strong, narrow Raman lines are observed in the crystal and the glass [14-16]. Raman-scattering spectra of amorphous and single-crystal germanium di-chalcogenides at high pressures have been reported [17, 18]. K. Murase et al. [17] found that there is no change in the frequencies of the A_1 and A_{1c} modes in a-$GeSe_2$ up to 2GPa. In the case of $GeSe_2$ single crystal, as the pressure increases to 5GPa, a splitting appears of the highest intensity mode at 211cm^{-1}.

Chalcogenide semiconductors usually show photoluminescence (PL) spectra with large Stokes shift. In the case of a typical chalcogenide semiconductor $GeSe_2$ the excitation by near or above band gap light (~ 2eV) causes a Gaussian shaped photoluminescence spectrum with ~ 0.3eV full width at half maximum (FWHM) amplitude at around 1eV for both crystalline and glassy forms [19-21].

It is very important for luminescence research to find systems in which the emitted light lies in the visible region. The emitted luminescence spectra favorite some rare earth compounds to be used as laser materials, lamp phosphors or

as x-ray phosphors [22-24]. In particular Gd^{3+} compounds are interesting from a fundamental and a practical point of view [25]. Gd^{3+} activated phosphors have attracted much attention for their well defined emission in the ultraviolet region [14, 26, 27].

Recently, Pr^{3+}- or Dy^{3+}- doped selenide glasses with much lower phonon energy have also been investigated and favorable 1.3μm emissions have been observed [28]. Yet now, all Raman and PL investigations have been performed for Ge-Se system in the glassy and crystalline states. No previous research were applied to Ge-Se in the nano-crystal scale which due to confinement affects open the door to more available and interesting characteristics. Moreover, doping with rare earth elements has been rarely studied. In this work we present new diagnostic Raman and PL data on nano-crystalline $GeSe_2$ and $GeSe_2$:Gd. From absorbance measurements a wide optical band gap of 4.8 for the doped sample is reported. New Raman activities and PL emission bands were recorded for virgin and Gd-doped samples over the visible range. The main objective for the present work is the development of visible source based on the radiative transition of Gd^{3+} in nano-crystalline $GeSe_2$.

2. Experimental Work

$GeSe_2$ and $Ge_{0.7}Se_2Gd_{0.3}$ were prepared by direct fusion of highly pure elements: Geshot (99.999%), Se shot (99.999%), and Gdpowder (99.999%) produced by Aldrich Chem. Co. Inc. The necessary quantities of the elements required for the preparation of an ingot of 7 gm were weighed according to their atomic weights using an electrical sensitive microbalance of accuracy 10^{-4} gm. The weighed elements were transferred to pre-cleaned quartz tubes (diameter = 2 cm and length= 20 cm). The tubes were then sealed under vacuum of 10^{-4}Torr. Heatingup to 1000°C was carried out. The furnace temperature was maintained at 1000°C for 72 h. During the synthesis process, the molten tubes were occasionally shaken to ensure homogeneous mixing of the constituents. The molten tubes were allowed to cool inside the oven down to room temperature. X-ray diffraction using Philips diffractometer (X'pert MPD) goniometer type PW3050/10 with Cu-Kαradiationwas elaborated. The crystal structure (lattice parameters, atomiccoordinates, occupancy factors, displacement factors) and microstructure (crystallite sizes (D_F)) and r.m.smicrostrain(e_g) wererefined applying Rietveld profile method using MAUD and WinFit programs[29]. Absorbance measurement was carried out by using Perkin-Elmer Spectrophotometer, model lambda 35 in the UV/Visible spectral range. Raman spectrometer (Bruker) was used for Raman investigation. Calibration is done automatically by the instrument with Neon lamp. This instrument is characterized by the removal of fluorescence background and high wave number accuracy. The laser wavelength 532-785nm, laser characteristics (lasing medium) AlGaAs (laser type) semiconductor and the spot size of laser is 20xobjective $4x10^{-12}$($4\mu m^2$). All spectra were recorded at room temperature under similar spectral parameters. The Perkin Elmer Ls55 florescence spectrometer used to measure Photoluminescence intensity of the samples has holographic gratings to reduce stray light, as well as automated polarizers. Ls55 uses a high energy pulsed Xenon source for excitation and has a wide wavelength rang 200-900nm. The advantages of this source are the minimal photo bleaching of samples and the improved low light detection capability relative to other light sources.

3. Results and Discussion

3.1. Structure and Microstructure

The X-ray diffraction patterns of $GeSe_2$ and $Ge_{0.7}Se_2Gd_{0.3}$ are shown in Fig. 1. The search-match program showed no diffraction lines related to the elements or their oxides; only one phase of $GeSe_2$ was present according to the ICDD card number (71-0117)with the monoclinic space group $P2_1/c$. During Rietveld analysis, a preferred orientation along the [0 0 ℓ] direction was detected. The latter could not be avoided during measurements in spite of back-loading and fine grinding of samples. This preferred orientation is mainly due to the presence of the stacking layers aligned on the top of each other along the [0 0 ℓ] direction [30]. Fig. 2(a, b) shows the profile fitting resulting from the structure refinement of the two compounds under study. The structural parameters obtained from Rietveld refinement are shown in Table 1.

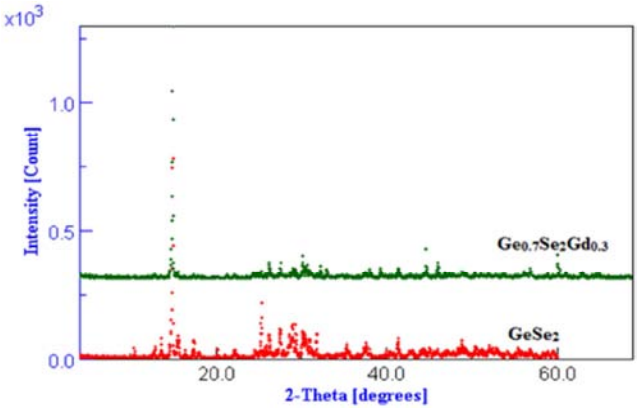

Fig. 1. *X-ray diffraction patterns of $GeSe_2$and $Ge_{0.7}Se_2Gd_{0.3}$.*

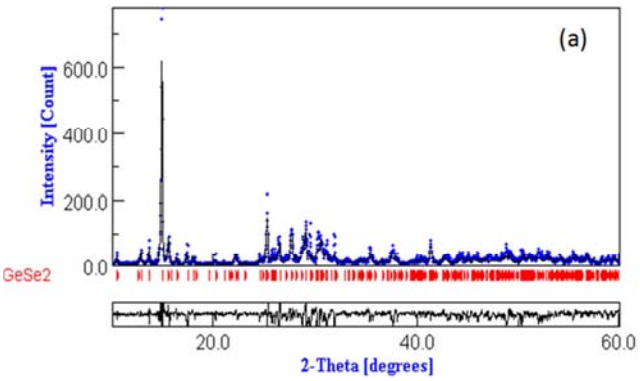

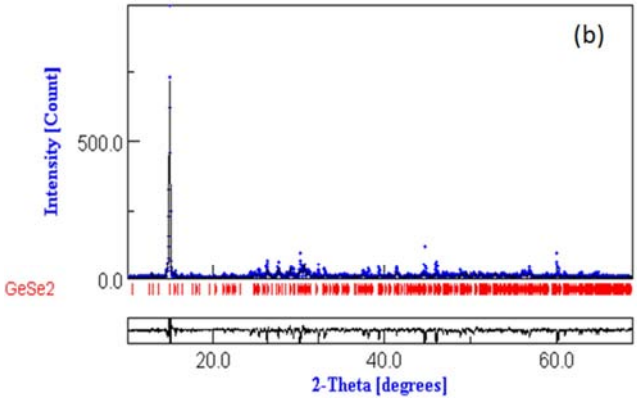

Fig. 2. *The profile fitting of (a)$GeSe_2$ and (b)$Ge_{0.7}Se_2Gd_{0.3}$.*

The results of WinFit Single Line Analysis (S.L.A) and Multiple Line Analysis (M.L.A) of the prepared compounds are given table 1. The prepared samples exhibit monoclinicnano-crystalline structure. Doping with Gd causes an increase of crystallite size (D_F) by 16.5% with respect to $GeSe_2$due to the big atomic radius of Gd. It is to be noted also that the value of $<e_g>$ is approximately doubled.

Table 1. *The structural parameters of the systems.*

parameter	$GeSe_2$	$Ge_{0.7}Se_2Gd_{0.3}$
a (A°)	7.0809	7.0736
b (A°)	16.8458	16.7568
c (A°)	11.8494	11.8806
R_W (%)	11.2	10.8
R_P (%)	10.7	9.3
(S.L.A) D_β(nm)	40.7	43.3
D_F(nm)	44.9	46.5
(M.L.A) D_β(nm)	40.2	46.7
D_F(nm)	41.1	47.9
$<e_g>$ of 00ℓ	0.019%	0.0415%

3.2. Absorbance Measurements

To investigate the optical properties of nano-crystalline $GeSe_2$:Gd, the UV-Vis.absorption spectra were followed for the samples in the form of grinded powder dispersed in distilled water. The obtained data of $GeSe_2$ and $Ge_{0.7}Se_2Gd_{0.3}$ are given in Fig. 3. The optical absorption edge was determined by drawing straight line through the sharp edge. The intersection with the abscissas taken as the value of the optical gap (E_g), so E_g could be estimated to be about 4.1eV for $GeSe_2$ and 4.8eV for $Ge_{0.7}Se_2Gd_{0.3}$. These large values of E_g with respect to bulk amorphous $GeSe_2$(2.14eV) [31] are due to the quantum confinement effect because of thenano-nature of the crystallite size. It is evident that doping with Gdincreases the width of the forbidden band gap. This is probably due to the strong cohesive energy of Ge-Gd and Se-Gd bonds with respect to Ge-Se bond.

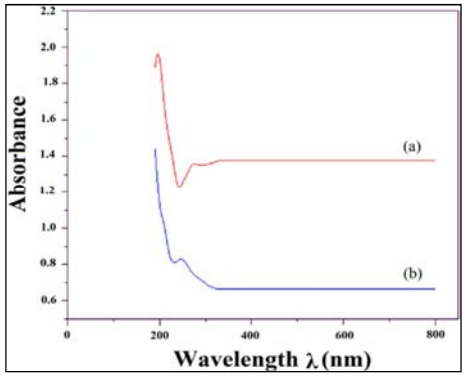

Fig. 3. *Wavelength versus absorbance for (a) $GeSe_2$and (b) $Ge_{0.7}Se_2Gd_{0.3}$.*

3.3. Raman Investigation

Fig. 4(a,b) shows the Raman spectra for the virgin and Gd-dopednano-crystalline samples. We have performed curve fitting procedure on the experimental high resolution Raman spectra using independent Gaussian function. The deconvolutedspectra are also illustrated. The Raman activities, peak position, full width at half maximum (FWHM) and their relative intensities are listed in table 2. As clearly seen, for nano crystalline $GeSe_2$, the main vibrational mode is centered at 202.08cm^{-1} (Peak 5) in addition to four lower intensity bands at the left and the right sides of the main band.

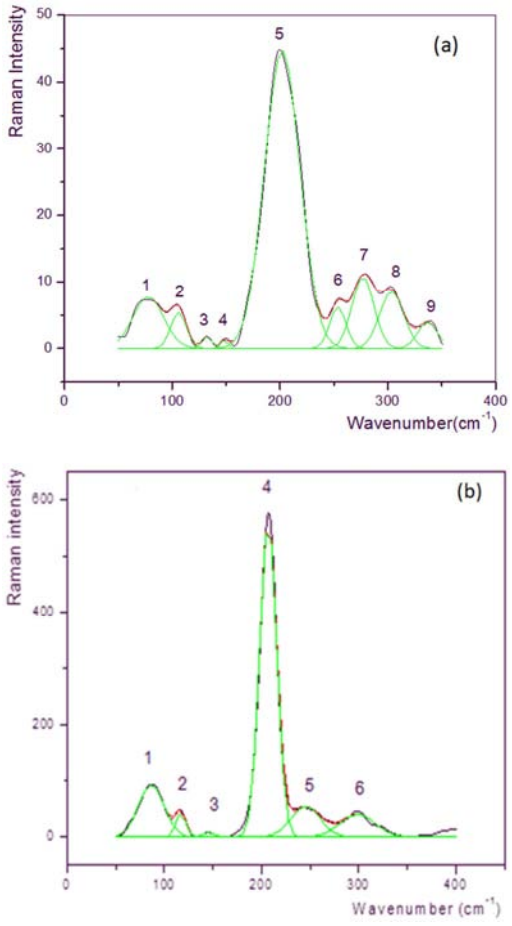

Fig. 4. *Raman spectra of (a) $GeSe_2$ and (b) $Ge_{0.7}Se_2Gd_{0.3}$.*

Table 2. *The Raman activities, peak position, FWHM and relative intensities for $GeSe_2$ and $Ge_{0.7}Se_2Gd_{0.3}$.*

Peak	$GeSe_2$			$Ge_{0.7}Se_2Gd_{0.3}$		
	Position	FWHM	Intensity	Position	FWHM	Intensity
1	77.774	28.531	7.7083	86.599	26.176	93.490
2	105.87	14.238	5.4150	116.93	10.232	43.541
3	132.19	8.5222	1.8569	145.65	11.453	8.5930
4	148.51	6.0726	1.3667	206.87	17.216	566.25
5	202.08	32.874	44.810	245.27	30.454	54.497
6	253.67	14.971	6.2837	298.7	36.195	40.405
7	277.01	20.195	10.739	-	-	-
8	303.64	22.069	8.6006	-	-	-
9	336.91	18.181	3.9459	-	-	-

Earlier reports for crystalline $GeSe_2$ shows two strong Raman bands at υ_1=210.3cm^{-1} with FWHM = 3.0±0.2cm^{-1} and at υ_2=215.4±0.5cm^{-1} with FWHM = 3.2±0.4cm^{-1} [32]. The authors reported that these FWHM are considerably narrower than the corresponding Raman bands of the glassy format υ_1=198cm^{-1} and υ_2=212cm^{-1} [33]. Similar bands in crystalline $GeSe_2$ at 210.4cm^{-1} and 216 cm^{-1}were also reported by T. Nakaoka et al. [34]. In our case, the Raman analysis of the nano-crystalline $GeSe_2$ shows only one strong mode at 202.08cm^{-1}. The splitting of the A_1 (symmetric tetrahedral breathing) Raman mode reported for both crystalline and glassy $GeSe_2$ is completely absent as shown in Fig. 4. The absence of the splitting of the main mode in the present study could be a result of a superposition of the A_1 vibration of corner sharing $GeSe_4$ tetrahedra and the A_{1C} vibration of edge sharing $GeSe_4$ tetrahedra that appear at very close frequency and has intensity lower than the first one.

The result of curve fitting of Raman spectra at 202cm^{-1} of Ge-Se cluster model of R. Holomb et al. [35] indicates that, the peak located at ~ 204.1cm^{-1} is in very good accordance with the Raman mode at 204/205cm^{-1} calculated for six-membered rings and larger ring like Ge_nSe_m cluster topologically similar with the high temperature (HT) $GeSe_2$.

An anomalous feature characterizes the nano-crystalline $GeSe_2$ under study with respect to glassy $GeSe_2$ is the existence of well identified low intensity Raman modes at low frequencies υ < 145cm^{-1}. The spectral ranges from 30-150 cm^{-1} are attributed to the bond-bending vibrations in layered structure materials [18]. On the other hand the clearly observable four high frequency modes shown in Fig. 4(a) at υ >250cm^{-1} were also reported by Z. V. Popovic et al. [36], while studying the Raman scollering spectra of the β-modification of $GeSe_2$ under hydrostatic pressure. The authors observed that as the pressure increases, the high temperature (HT) layered structure of $GeSe_2$ undergoes a transformation to low temperature (LT) modification with preserving the modes at 275 $cm^{-1}$and 304 cm^{-1}.

In Fig. 4(a), the existence of the modes at 277.01 cm^{-1} and 303.64 cm^{-1} gives evidence that, the nano-crystalline $GeSe_2$ under study exhibits the LT structure in which the $GeSe_4$ tetrahedra are connected via common corners.

Raman spectra are also manipulated to determine the local environment of Gd^{3+} in the $GeSe_2$ host lattice. As given in Fig. 4(b) and table 2, doping the nano-crystalline $GeSe_2$ with Gd, considerably affect the Raman vibration spectrum of the virgin sample and hence the local environment of the existing atoms as the nine lines recorded for $GeSe_2$ (table 2) are reduced to six lines only. The principle band at 202.08 cm^{-1} is shifted to higher energies (206.87 cm^{-1}), its FWHM is decreased by ~ 50% and its intensity increased by ~ 17.2 fold times with respect to that of the pure sample. The stronger band near 206 cm^{-1} in nano-crystalline $Ge_{0.7}Gd_{0.3}Se_2$ can be attributed to the overlap of υ_1 (A_1) symmetric stretching modes of corner-shoring $GeSe_4$ and $GdSe_4$ tetrahedral, the increased intensity detected for Gd-doped sample can be assigned to more formation of such structure building unit. Further theoretical calculations are needed for the assignment of Raman modes of this nano-chalcognide material to determine the local environment of Gd^{3+} in the $GeSe_2$ host lattice.

3.4. Photoluminescence (PL) Investigation

The observed PL spectra for nano-crystalline $GeSe_2$ and $Ge_{0.7}Se_2Gd_{0.3}$ are shown in Fig. 5 (a,b). These spectra were obtained using excitation energy of 2.69eV. Curvefitting procedure was applied to the experimental spectra using independent Gaussian function. The recorded emission bands are given in table 3. As shown, over the visible region, the major emission is located at 604.33nm (2.05eV) accompanied by a shoulder at 617.37nm (2.01eV) in addition to less intensity line at 551.9nm (2.25eV).

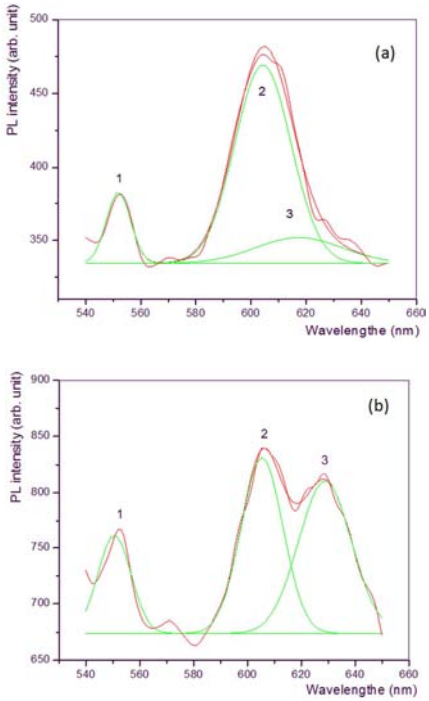

Fig. 5. *PL spectra for nano-crystalline (a) $GeSe_2$ and (b) $Ge_{0.7}Se_2Gd_{0.3}$.*

Table 3. *The recorded emission bands for nano-crystalline $GeSe_2$ and $Ge_{0.7}Se_2Gd_{0.3}$.*

Peak	$GeSe_2$			$Ge_{0.7}Se_2Gd_{0.3}$		
	Position	FWHM	Intensity	Position	FWHM	Intensity
1	551.90	8.7547	48.567	550.63	12.248	87.101
2	604.33	20.402	135.26	605.44	15.504	157.68
3	617.37	31.504	17.493	628.83	19.500	136.56

Photoluminescence studies on melt-quenched Ge_xSe_{1-x} ($0.2 < x < 4.3$) glasses revealed the presences of a broad peak with a maximum located at about half the band-gap energy (~1.1eV) for $GeSe_2$ when the excitation is 2.335eV [37]. Also, M. Koos et al. [38] predicteda peak at 1.17eV for glassy $GeSe_2$. Annealing at 573^{o}K shifts the peak towards higher energies by about 0.1eV thus corresponds roughly to the value recorded for crystalline $GeSe_2$.

In our case for nano-crystalline $GeSe_2$, the measured optical band gap (Fig. 3) is ~ 4.1eV, so the PL emission band recorded at ~2.05eV (604.33nm) can be attributed to band-band transition. The other higher energy (2.25eV) emission is probably created through transition between valance-band states up to states into the conduction-band caused by free electrons.

Fig. 5(b) gives the emission spectrum for nano-crystalline $Ge_{0.7}Se_2Gd_{0.3}$ sample. As shown in the figure, the major band with its shoulder detected for virgin sample is splitted into two intense bands by introducing Gd as a rare earth atom. The position, the intensity and FWHM of the emission bands are given in table 3. It is to be noted that, the intensities of all emission bands are nearly doubled by Gd incorporation.

The results reported by Kastner and Hudgens [39] have been interpreted as showing that the radiative centers in chalcogenides are neutral dipole centers (i.e closely situated charge pairs) rather than randomly distributed charge ones. According to Kastner and Fritzsche [40], the density of intimate pairs is independent of doping up to concentrations characteristic of alloying i.e.PL would be insensitive to doping. If doping were to substantially alter the concentration of singly coordinated centers (D^-) or three-fold coordinated (D^+) centers (the famous defects in disordered chalcogenide semiconductors) or their relative density then a change in PL bands could be expected, provided that one or both these defects acted as radiative centers [38].

According to the emission spectra of Gd^{3+}(Fig.6), one can assign the bands at wave number > 550 cm^{-1} to transitions from ^6G_J to the different ^6P_J terms.

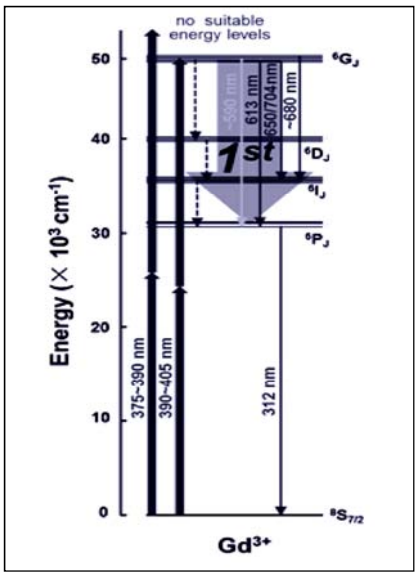

Fig. 6. *Energy spectra of Gd^{3+}.*

No previous investigation using PL have been carried out in Gd doped $GeSe_2$ so it was difficult to compare the recorded emission bands with other works to determine precisely the corresponding energy levels of Gd. R. T. Wegh et al. [41] reported first results on Gd^{3+} to study the luminescence of rare earth ions under vacuum ultraviolet (UVU) excitation. The author reported that the detected emissions at 577.6 nm, 606.7 nm and 631.2nm are assigned to $^6G_J \rightarrow {}^6P_J$ transitions of Gd^{3+}. Brixner and Blasse [42] were the first to observe $^6G \rightarrow {}^8S$ emission of Gd^{3+} in several host lattices at higher energies at about 205and 186nm. Other experimental and theoretical works are necessary to confirm the possibility of using nano-crystalline $GeSe_2$ doped with Gd as a radiative visible source.

4. Conclusion

First optical properties through Raman and photoluminescence studies are performed for nano-crystalline pure and Gd-doped $GeSe_2$. New results, with comparison to glassy and crystalline $GeSe_2$, are given. Doping with Gd is found to alter the local environment of the existing atoms as predicted by Raman and PL analysis. The assignment of Raman emission lines and energy level transitions of Gd^{3+} in the host $GeSe_2$ are suggested.

Acknowledgements

The author is indebted to Prof. Dr. K. Sedeek for guidance and useful discussion during this work. The author is grateful to the Grants Commission of Al-Azhar University –Cairo – Egypt for supporting this work. The author is also thankful to X-ray Diffraction unit, Inorganic chemical laboratory, Ain-Shams University and Petroleum research center for extending the X-ray, PL and Raman facility.

References

[1] R. M. Almeida, L. F. Santos, A. Simens, A. Ganjoo and H. Jain, J. Non-Cryst. Solids, 353(2007) 2066.

[2] H. Nicolas, J. M. Laniel, R. Valle and A. Villeneuve, Opt. Lett, 28(2003) 965.

[3] W. J. Miniscalco and M. J. F. Digonnet (Ed.), Rare Earth Doped Fiber Lasers and Amplifiers, Marcel Dekker, New York, (1993) 35.

[4] L. Russo, M. Vlcek and H. Jain, Glass Technol, 46(2005) 94.

[5] K. Tanaka, J. Non-Cryst. Solids, 352 (2006) 2580.

[6] L. A. Wahab, A. Adam, M. R. Balboul, N. Makram, A. A. El-Ela and K. Sedeek, J. Physica B, 387 (2007) 81.

[7] K. Sedeek, M. Fadel and M. A. Afify, J. Mater. Sci, 33 (1998) 4621.

[8] S. R. Elliot and A. T. Steel, J. Phys. Rev. Lett, 57 (1986) 1316.

[9] K. Sedeek, J. Phys. D: Appl. Phys, 26 (1993) 130.

[10] T. Schweizer, D. W. Hewak, B. N. Samson and D. N. Payne, J. Lumin, 72±74 (1997) 421.

[11] S. Tanabe, T. Hanada, M. Watanabe, T. Hayashi and N. Soga, J. Am. Ceram. Soc, 78 (1995) 2917.

[12] R. Reisfeld, Ann.Chim.Fr, 7 (1982) 147.

[13] B. Cole, L. B. Shaw, P. C. Pureza, R. Mossadegh, J. S. Sanghera and I. D. Aggarwal, J. Non-Cryst. Solids, 256&257 (1999) 253.

[14] P. Tronc, M. Bensoussan, A. Brenac and C. Sebenne, J. Phys. Rev. B, 8 (1973) 5947.

[15] R. J. Menanich and S. A. Solin, Commun, 21 (1977) 273; R. J. Nemanich, Phys. Rev. B, 16 (1977) 1655.

[16] Z. V. Popovic and P. M. Nikolic, J. Solid State Commun, 27 (1978) 561.

[17] K. Murase, T. Fukunago, P. C. Taylor (Ed.) and S. G. Bishop (Ed.), Optical Effects in Amorphous Semiconductours, AIP Conf. Proc. No.120 (AIP, New York, 1984) 449.

[18] Z. V. Popovic, Z. Jaksic, Y. S. Raptis and E. Anastassakis, J.Phys.Rev.B, 57 (1998) 3418.

[19] V. A. Vassilyev, M. Koo´s and I. K. Somogyi, Solid State Commun, 22 (1977) 633.

[20] V. A. Vassilyev, M. Koo´s and I. K. Somogyi, Philos. Mag. B, 39 (1979) 333.

[21] R. A. Street and D. K. Biegelsen, Solid State Commun, 32 (1979) 339.

[22] G. Boulon, J.Rev.Phys. Appl, 21 (1986) 689.

[23] G. Blasse, ed. Mat. Chem. Phys, 16 (1987) 3-371.

[24] A. J. De Vries, M. F. Hazenkamp and G. Blasse, J. Luminescence, 42 (1988) 275.

[25] G. Blasse, H. S. Kiliaan, A. J. de, Vries, J. Less-Common Met, 129 (1986) 139.

[26] K. N. Shinde, V. B. Pawade, S. J. Dhoble, A. Hakeem, Impact of temperatureon $Na_2Sr(PO_4)F:Eu^{3+}$ phosphor, Luminescence, 29(2014) 352–6.

[27] S. Tamboli, B. Rajeswari and S. J. Dhoble, J. Biological and Chemical luminescence, 13 (2016) 551.

[28] P. Neˇmec, B. Frumarova´, M. Frumar and J. Oswald, J. Phys. Chem. Solids, 61 (2000) 1583.

[29] P. Scardi, L. Lutterotti and P. Masitrelli, Powder Diff, 9(3) (1994) 180.

[30] K. El-Sayed, Z. K. Heiba, K. Sedeek and H. H. Hantour, J. Alloys and Comp, 530 (2012) 102.

[31] R. K. Pan, H. Z. Tao, H. C. Zang, X. J. Zhao and T. J. Zhang, J. Alloys and Comp, 484 (2009) 645.

[32] N. Kumagai, J. Shirafuji and Y. Inuishi, J.Phy.Soc.Jpn, 42 (1977) 1261.

[33] P. M. Bridenbaugh, G. P. Espinosa, J. E. Griffiths, J. C. Phillips and J. P. Remeika, Phys.Rev.B, 20 (1979) 4140.

[34] T. Nakaoka, Y. Wang, K. Murase, O. Matsuda and K. Inoue, Phys. Rev,61 (2000) 15569.

[35] R. Holomb, V. Mitsa, E. Akalin, S. Akyuz and M. Sichka, J.Non-Cryst.Solids, 373–374 (2013) 51.

[36] Z. V. Popovic and H. J. Stolz, J. phys. stat. sol. (b), 108 (1981) 153.

[37] R. A. Street and D. K. Biegelsen, J. Non-Cryst. Solid, 32 (1979) 339.

[38] M. Koos, I. Kosa Somogyi and V. A. Vassilyev, J. Non-Cryst. Solids, 43 (1981) 245.

[39] M. Kastner and S. J. Hudgens, Phil. Mag. B, 37 (1978) 665.

[40] M. Kastner and H. Fritzsche, Phil. Mag. B, 37 (1978) 199.

[41] R. T. Wegh and A. Meijerink, J.ActaPhysica A, 90 (1996) 333.

[42] L. H. Brixner and G. Blasses, J. Chem. phys. lett, 157 (1989) 283.